

Feshbach molecule formation through an oscillating magnetic field: subharmonic resonances

S. Brouard and J. Plata

*Departamento de Física, Universidad de La Laguna,
La Laguna E38204, Tenerife, Spain.*

Abstract

The conversion of ultracold atoms to molecules via a magnetic Feshbach resonance with a sinusoidal modulation of the field is studied. Different practical realizations of this method in Bose atomic gases are analyzed. Our model incorporates many-body effects through an effective reduction of the complete microscopic dynamics. Moreover, we simulate the experimental conditions corresponding to the preparation of the system as a thermal gas and as a condensate. Some of the experimental findings are clarified. The origin of the observed dependence of the production efficiency on the frequency, amplitude, and application time of the magnetic modulation is elucidated. Our results uncover also the role of the atomic density in the dynamics, specifically, in the observed saturation of the atom-molecule conversion process.

PACS numbers: 03.75.Nt, 34.50.-s, 34.20.Cf

I. INTRODUCTION

The optimization of the methods used for the production of ultracold molecules, in particular, the minimization of losses, is an objective of current research [1]. Magnetic-field variations across a Feshbach resonance (FR) [2–4] and photoassociation [5–7] are the techniques most frequently applied to molecule formation. In particular, linear magnetic ramps [3, 8–17] are standardly used in both Fermi and Bose gases. Additionally, Ramsey-like techniques, implemented via magnetic-field jumps close to a FR, have been applied to produce coherent superpositions of atoms and molecules [2, 18, 19]. Here, we focus on an alternative method based on a sinusoidal modulation of the field in a magnetic FR. This scheme was first realized in experiments on thermal and condensed gases of ^{85}Rb [20]. In them, a resonant behavior of the efficiency was observed at a modulation frequency matching the molecular binding energy. The experiments revealed also the nontrivial dependence of the efficiency on the application time of the perturbation: the molecule population presented damped oscillations in the initial stage followed by a slow growth, which, eventually, saturated. A preliminary analysis, based on a two-body model with a two-channel configuration, showed that the observed features could not be understood in terms of a Rabi-like oscillation. A more complete description, in particular, the inclusion of different sources of decoherence, was required [20]. Theoretical and experimental work followed. The role of the system preparation was analyzed [21]. It was shown that, for a thermal gas, the initial distribution of atomic states leads to a quasi-continuous set of oscillatory components in the evolution of the molecular mode, and, consequently, to dephasing. The confinement in an optical lattice was also considered [22]. A variation of the modulation technique [23], applied to a mixture of different atomic species, uncovered molecular production at subharmonics of the resonance frequency. A similar effect was found for a single atomic species [24]. Despite the advances, there are still open questions; here, to go further in the clarification of the physical ground of the method, we extend former work on its general characteristics. We evaluate the differential role of the essential components of the dynamics in the emergence of the observed features. First, from an analytical description, we identify the characteristics rooted in the two-body Hamiltonian dynamics. Then, multi-atomic effects are assessed through a nonlinear configuration-interaction approach. In this framework, we analyze the effect of losses. Finally, we deal with the implications of the system preparation. Our ap-

proach is primarily applied to the experiments of Ref. [20]. The different time-scales and the eventual saturation of the transfer are explained as a combined effect of decoherence and nonlinearity of the (reduced) multi-atomic dynamics. Moreover, we uncover the origin of the resonances observed at subharmonics of the molecular binding energy in Refs. [23] and [24]. A discussion of phase-space dependent restrictions to the efficiency, relevant to quite general contexts, is also presented.

The outline of the paper is as follows. A first model, which incorporates basic two-body aspects of the dynamics, is presented in Sec. II. In Sec. III, an (effective) nonlinear Rabi model is applied to deal with the multi-atomic characteristics of the process. Molecular decay is included in this approach. The experimental preparation of the system is simulated in Sec. IV. Finally, some general conclusions are summarized in Sec. V.

II. A TWO-BODY DESCRIPTION OF GENERAL DYNAMICAL CHARACTERISTICS

We consider a Bose gas of ultracold atoms in a weakly confining harmonic trap. It is assumed that, as in the mentioned experiments, the interaction strength is controlled by a time-dependent magnetic field via a FR. In the practical arrangements, the field was modulated as

$$B(t) = B_0 + B_m \sin(\omega t). \quad (1)$$

The average value B_0 was taken close to a FR position B_r . Additionally, in order to work in a perturbative regime, the modulation amplitude B_m was fixed at a sufficiently small value, $B_m \ll |B_0 - B_r|$. The experiments of Ref. [20] were carried out on ^{85}Rb . In Ref. [23], a similar magnetic-modulation technique was applied to a mixture of ^{41}K and ^{87}Rb . Instead of a detailed characterization of each scenario, we will build a general framework where the elements responsible for the diverse observed features can be identified. A local-density approximation is applicable to the usual experimental conditions. Here, we concentrate on the simplest case of a uniform system: we will show that, in it, some of the experimental findings can be reproduced. Consistently, the atomic energy levels, which are slightly spaced because of the weak trapping, will be approximated as a quasi-continuum.

A. The undriven system

Let us first consider the system without the magnetic modulation, (i.e., with $B_m = 0$.) The starting point in standard approaches is a description of the coupled atom-molecule system in terms of *bare states*, i.e., of the eigenstates in the absence of coupling [1]. The usual picture incorporates the (closed-channel) FR state $|R\rangle$, and coupled to it, the (entrance-channel) atom state $|S\rangle$. Correspondingly, the Hamiltonian reads $H_1 = H_0 + V$, where H_0 stands for the interaction-less system and V represents the coupling term. Thus,

$$\begin{aligned} H_0 |S\rangle &= E_S |S\rangle, & 0 \leq E_S < \infty, \\ H_0 |R\rangle &= -\epsilon_{B_0} |R\rangle, & \epsilon_{B_0} > 0, \\ \langle R| V |S\rangle &= v(E_S), \end{aligned} \tag{2}$$

where E_S denotes the energy along the atomic set and ϵ_{B_0} represents the binding energy of the state $|R\rangle$ at the mean magnetic field B_0 . By now, we assume that the interaction strength $v(E_S)$ hardly varies with E_S . Moreover, we consider that the set of eigenstates of the complete Hamiltonian H_1 , i.e., the *dressed states*, consists of a bound eigenstate $|M\rangle$, (the molecular state), with energy $-\epsilon_M$, and a continuum of states $|A\rangle$ with energy E_A . Hence,

$$\begin{aligned} H_1 |A\rangle &= E_A |A\rangle, & 0 \leq E_A < \infty, \\ H_1 |M\rangle &= -\epsilon_M |M\rangle, & \epsilon_M > 0. \end{aligned} \tag{3}$$

Both, $|M\rangle$ and $|A\rangle$, are given by superpositions of $|R\rangle$ and $|S\rangle$. For field values close to the resonance position, $|M\rangle$ can significantly differ from $|R\rangle$, and, in order to properly describe atom-molecule transfer processes, the dressed-state representation becomes necessary. This is the case of the considered situations: the resonant character of the modulation applied in the experiments refers specifically to the approximate matching of ϵ_M and $\hbar\omega$.

B. The driven system

In the practical setups [20], the magnetic field was connected through a *trapezoidal* ramp, as that outlined in Fig. 1. The first linear segment slowly drives the field from $B(t = t_i)$, (far

from the FR), to B_0 . In the central *plateau*, the modulation described by Eq. (1) is applied. Finally, a slow linear ramp drives $B(t)$ back to its original value. This arrangement demands the generalization of previous theoretical approaches. Accordingly, we develop a method which combines the following elements. First, an adiabatic approximation connecting the bare and dressed representations will be used in our simulation of the (slow) linear segments of
cond, in the central region,
on

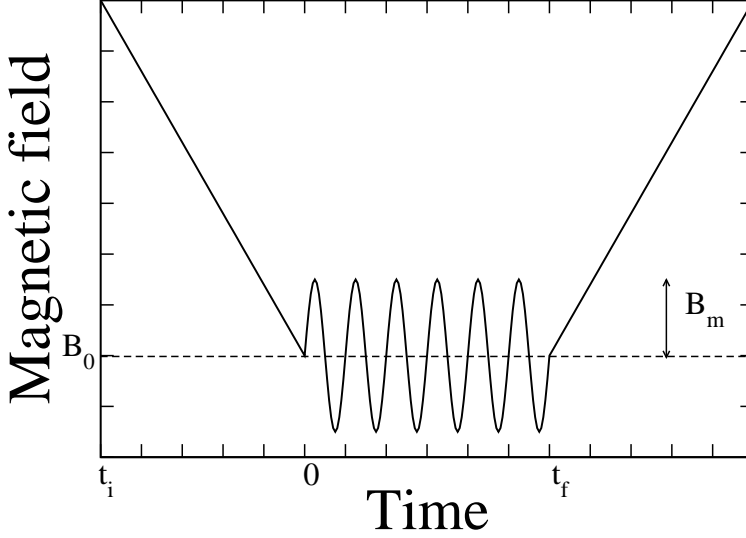


Figure 1: A diagram (with arbitrary scales) of the experimental magnetic-field ramp.

The modulation is straightforwardly included in the bare-state picture: we assume that the field variation merely alters ϵ_{B_0} , according to $\epsilon_{B_0} + \hbar C_{B_0} B_m \sin(\omega t)$, where $\hbar C_{B_0} = [\frac{\partial \epsilon}{\partial B}]_{B_0}$ is given by the difference between the magnetic moments of the involved states. (We will take $\hbar = 1$.) Hence, the driven system is described by the Hamiltonian $H_2 = H_1 + C_{B_0} B_m \sin(\omega t) |R\rangle \langle R|$, which, in the basis of dressed states is written as

$$\begin{aligned}
H_2 = & [-\epsilon_M + \eta_M \sin(\omega t)] |M\rangle \langle M| + \\
& [E_A + \eta_A(E_A) \sin(\omega t)] |A\rangle \langle A| + \\
& [v_{eff}(E_A) \sin(\omega t) |M\rangle \langle A| + \text{h.c.}],
\end{aligned} \tag{4}$$

where $\eta_M = C_{B_0} B_m |\langle M| R\rangle|^2$, $\eta_A(E_A) = C_{B_0} B_m |\langle A| R\rangle|^2$ and

$$v_{eff}(E_A) = C_{B_0} B_m \langle M| R\rangle \langle R| A\rangle. \tag{5}$$

The perturbation, apart from introducing a time-dependent coupling between the states $|M\rangle$ and $|A\rangle$, leads to a time variation in their *eigenenergies*. Furthermore, it can also couple different $|A\rangle$ states. However, that induced interaction between dressed atom states is neglected because of the small magnitude of the involved state-projections and the fact that the driving field and the atomic energy spacing are far from resonance.

A comparison with the Landau-Zener (LZ) model [25, 26], used to describe molecule production and dissociation induced by linear ramps, is of interest. In the LZ approach, the linear variation of the energy mismatch between the (*adiabatic*) bare states leads to the eventual occurrence of a level crossing. In contrast, in our approach, the (sinusoidal) perturbation is not large enough for leading to crossings. In both models, the ramp starts and ends sufficiently far from the FR for the bare states to be approximate eigenstates at the extremes. As opposed to the standard solving method of the LZ model, our approach requires the switch to the dressed description. We will see that many-body effects can be included in our description in a form similar to that used in the counterpart generalization of the LZ model [26, 27].

C. The secular dynamics

We tackle the dynamics by applying the unitary transformation

$$U(t) = e^{i\left[l\omega t + \frac{\eta_M}{\omega} \cos(\omega t)\right]|M\rangle\langle M| + \frac{\eta_A}{\omega} \cos(\omega t)|A\rangle\langle A|} \quad (6)$$

where $l(>0)$ is the nearest integer to the quotient between ϵ_M and ω . No restrictions on the perturbation frequency are assumed by now: the value of ω that optimizes the conversion will be determined in the following analysis. (Our study is not limited to the spectral region corresponding to $l = 1$: we will also deal with frequencies quasi-resonant with fractional values of ϵ_M [23, 24].) The transformed Hamiltonian $H'_2 = U^\dagger H_2 U - iU^\dagger \dot{U}$ reads

$$H'_2 = (-\epsilon_M + l\omega) |M\rangle\langle M| + E_A |A\rangle\langle A| + v_{eff} \sin(\omega t) \left[|M\rangle\langle A| \sum_{k=-\infty}^{\infty} (-i)^k J_k(\zeta/\omega) e^{-i(k+l)\omega t} + \text{h.c.} \right], \quad (7)$$

where $J_k(x)$ denotes the ordinary Bessel functions [28] and $\zeta = \eta_M - \eta_A = C_{B_0} B_m (|\langle M|R \rangle|^2 - |\langle A|R \rangle|^2)$. This Hamiltonian provides a framework for simplifying the

description; specifically, an analytical coarse-grained picture of the dynamics can be derived through the averaging of H'_2 . The effective detuning $-\epsilon_M + l\omega$ has been minimized by the choice of l as the nearest integer to ϵ_M/ω . (Later on, the displacement of the resonances by thermal effects will be evaluated.) H'_2 has a series of interaction terms oscillating with frequencies $(k+l\pm 1)\omega$, $k \in Z$. The secular dynamics is then governed by the components with $k = -l \mp 1$. The terms with $k \neq -l \mp 1$, barely affect the system evolution: they present fast oscillations, which, because of the small magnitude of their amplitudes compared with the involved frequencies, can be averaged out to zero. Hence, in the optimum frequency range, namely, for $l\omega \sim \epsilon_M$, the dynamics is approximately described by the effective Hamiltonian

$$H_{eff}^{(l)} = \delta^{(l)} |M\rangle \langle M| + E_A |A\rangle \langle A| + \left[\tilde{v}_{eff}^{(l)}(E_A) |M\rangle \langle A| + \text{h.c.} \right], \quad (8)$$

where $\delta^{(l)} \equiv l\omega - \epsilon_M$, and

$$\tilde{v}_{eff}^{(l)} \equiv -\frac{i^l}{2} [J_{-l-1}(\zeta/\omega) + J_{-l+1}(\zeta/\omega)] v_{eff} \quad (9)$$

is a *renormalized* coupling constant which incorporates the magnetic modulation. This picture provides the following clues to a preliminary understanding of some of the experimental results.

i) Each value of l defines a resonance, $-\epsilon_M + l\omega = 0$, around which, the dynamics is governed by a different effective Hamiltonian. The associated description corresponds to a discrete state coupled to a quasi-continuum. It can be anticipated that, for each $H_{eff}^{(l)}$, the transfer of population becomes more effective as the detuning decreases, which is consistent with the observed quasi-resonant character of the conversion process.

ii) From the properties of the Bessel functions, it follows that the relevance of the interaction term in the different $H_{eff}^{(l)}$ decreases as l grows. (This is particularly evident through the approximation $\tilde{v}_{eff}^{(l)} \simeq -\frac{i^l}{2} J_{-l+1}(\zeta/\omega) v_{eff}$, valid for small $|\zeta/\omega|$, as corresponds to the practical conditions.) These results agree with the findings of Ref. [23]. There, the production of molecules was observed to present different maxima at frequencies approximately given as $\omega \simeq \epsilon_M/l$, ($l \geq 1$), the heights of the maxima decreasing with l . Similar features were found in Ref. [24].

iii) Some comments on the dependence of $\tilde{v}_{eff}^{(l)}$ on the system parameters are in order. Let us illustrate the discussion by focusing on $\tilde{v}_{eff}^{(1)}$, which corresponds to the condition $\omega \simeq \epsilon_M$. In the perturbative regime, ($C_{B_0}B_m \ll \omega$), the effective coupling strength, given by Eqs. (5) and (9), can be approximated as

$$\tilde{v}_{eff}^{(1)} \simeq -\frac{i}{2}J_0(\zeta/\omega)C_{B_0}B_m \langle M| R \rangle \langle R| A \rangle. \quad (10)$$

The factor $J_0(\zeta/\omega)$ does not incorporate significant variations with the system parameters: it does not appreciably differ from unity, as can be seen through the approximation $J_0(\zeta/\omega) \simeq 1 - \frac{1}{4}(\zeta/\omega)^2$, valid for small arguments. Hence, $\tilde{v}_{eff}^{(1)}$ is determined by B_m and by C_{B_0} , and, also, by the product of state projections $\langle M| R \rangle \langle R| A \rangle$. In particular, $\tilde{v}_{eff}^{(1)}$ depends on B_0 , not only through C_{B_0} , but also via $\langle M| R \rangle \langle R| A \rangle$. These conclusions are consistent with the results presented in Ref. [29]. There, as the mean magnetic field B_0 was varied, (and, in turn, C_{B_0} was changed), the behavior of the coupling strength was observed to significantly depart from the mere linear dependence on $C_{B_0}B_m$. (For the terms with $l > 1$, the contribution of the factors that contain the Bessel functions can be nontrivial.)

iv) No phenomenological approaches have been made in our identification of the mechanism responsible for molecule production. The atom-molecule interaction induced by the magnetic driving has been traced in our first-principle scheme. However, the specific form of the effective Hamiltonians is strictly valid for small amplitudes and for frequencies in the quasi-resonant ranges. Outside those regimes, the applied approximation can break down, and, it is necessary to go back to H'_2 in Eq. (7) to have an appropriate description of the dynamics. In fact, given the nontrivial dependence of H'_2 on ω and B_m , qualitatively different responses can be expected from significant variations in those parameters.

The descriptions corresponding to the different effective Hamiltonians are parallel. Henceforth, we will focus on the dominant term $H_{eff}^{(1)}$, which will be simply denoted as H_{eff} . Moreover, we write $\delta^{(1)} \equiv E_M$ and $\tilde{v}_{eff}^{(1)} \equiv \tilde{v}_{eff}$. Therefore, the two-body dynamics of our system will be assumed to be governed by

$$H_{eff} = E_M |M\rangle \langle M| + E_A |A\rangle \langle A| + [\tilde{v}_{eff}(E_A) |M\rangle \langle A| + \text{h.c.}] \quad (11)$$

The quasicontinuum structure can be incorporated into the model by describing the

atomic set in terms of the density of states and the coupling function. Note first that the possibility of varying ω allows a certain degree of control over the role of the continuum: different positions of $|M\rangle$ with respect to the atomic border, ($E_M = \omega - \epsilon_M \gtrless 0$), can be realized by changing ω . For those different cases, the damping and energy shift of the discrete state are evaluated [30]. The results show that the features that we intend to explain, e.g., the different time scales or the saturation of the molecular population, do not seem to be rooted in damping due to the compact atomic-set structure. Therefore, we must explore alternative mechanisms: in the rest of the paper, we will evaluate the role of losses and many-body physics. Since we will neglect damping associated to the continuum structure, Eq. (11) will be regarded as defining an effective (linear) Rabi model involving $|M\rangle$ and an (isolated) generic state $|A\rangle$. This effective discretization implies the modification of the coupling constant to incorporate the characteristics of the density of states and the confining volume \mathcal{V} . The specific form of the resulting dependence of the interaction strength on \mathcal{V} is crucial to the role of the atomic density in the process. This issue was analyzed in Ref. [26] for a generic confinement. The results are applicable to our system: following them, we incorporate into Eq. (11) a modified coupling constant which depends on $\mathcal{V}^{-1/2}$. [For simplicity, we maintain the notation $\tilde{v}_{eff}(E_A)$.] In our reduced description of the atomic states, the variation of the energy E_A along the set is still contemplated.

III. A NONLINEAR CONFIGURATION-INTERACTION APPROACH TO THE MULTI-ATOMIC DYNAMICS

We turn to discuss how the above description can be generalized to study the multi-atomic scenario considered in the experiments. The generalization is necessary, in particular, for analyzing the dependence of the conversion efficiency on the atom density.

A first-principle description of many-body effects is out of the scope of the study. Instead, we have opted for an effective reduction of the microscopic dynamics. From a qualitative picture, we can identify two elements that must be incorporated into the generalization of the two-body approach. First, we must address *bosonic stimulation*: since, for a condensate preparation, each of the N identical atoms can interact with $N - 1 \simeq N$ others to form the molecular species, a scaling of the interaction strength in the equations for the populations is pertinent. Second, the appropriate *renormalization* of the dynamical equations cannot

be simply implemented by introducing an N dependent amplification factor in the coupling constant. The correct procedure should account for the changing number of single atoms in the system as the conversion progresses. The inclusion of an effective interaction strength which depends on the atomic population implies the use of nonlinear equations, where unitarity in the evolution of the populations must be maintained.

The methodology outlined above has been applied in previous studies. In early descriptions of transfers induced by linear ramps, the multi-atomic character was tackled by scaling the interaction strength in the equations obtained within a (standard) two-body LZ model. Specifically, in the expression $\left|C_M^{(as)}\right|^2 \simeq 1 - \exp(-w_{LZ})$, which gives the asymptotic molecular population in the standard approach, the LZ parameter w_{LZ} was replaced by Nw_{LZ} [26]. [w_{LZ} grows with the inverse ramp speed. In the adiabatic limit, where $w_{LZ} \rightarrow \infty$, the model predicts a complete transfer of population. Furthermore, since w_{LZ} scales also with the squared coupling matrix element, (and, in turn, with the inverse volume $1/\mathcal{V}$), the effective parameter Nw_{LZ} grows linearly with the atomic density N/\mathcal{V} .] In subsequent studies, it was also taken into account that the interaction strength changes as the molecular generation proceeds [27]: a *nonlinear* configuration-interaction LZ model was implemented.

Since the time scale for molecular decay is smaller than that of the complete conversion process, our model must also incorporate losses. Some numerical values illustrate this argument: whereas the saturation of the process was found to occur on a scale larger than 20 ms [20], a typical time for molecular decay was estimated to be of the order of 1 ms [31]. Loss mechanisms will be incorporated in a phenomenological way: we will describe them as a depletion of the molecular population characterized by the rate constant γ [23].

Following the above lines, we assume that the state of the system, expressed as $|\Psi(t)\rangle = C_A(t)|A\rangle + C_M(t)|M\rangle$, evolves according to a damped *nonlinear* Rabi model, built by extending the description given by Eq. (11), and explicitly defined by the set of equations [1, 32]:

$$\dot{C}_A = i\frac{\Delta}{2}C_A - \frac{i}{2}\Omega(N)C_A^*C_M \quad (12)$$

$$\dot{C}_M = -i\frac{\Delta}{2}C_M - \frac{i}{2}\Omega^*(N)C_A^2 - \gamma C_M, \quad (13)$$

where $\Delta \equiv E_M - E_A = \omega - (\epsilon_M + E_A)$ and $\Omega(N) \equiv \sqrt{N}\tilde{v}_{eff}$. Since $|\tilde{v}_{eff}|^2$ is proportional to the inverse volume, $|\Omega(N)|^2$ scales with the atomic density. Further on, to deal with a

thermal gas, where no bosonic stimulation takes place, we will be back to the framework defined by Eq. (11). By now, in order to concentrate on the features specifically rooted in the preparation as a condensate, we consider the system in a pure dressed atomic state $|A\rangle$, i.e., we take $C_A(0) = 1$, and calculate $|C_M(t)|^2$.

A. The undamped nonlinear Rabi oscillations

For $\gamma = 0$, analytical solutions to the above set of equations can be obtained [33]: the molecular population can be expressed in terms of the Jacobi elliptic function $\text{sn}(x, n)$ [28] as

$$|C_M(t)|^2 = p_1 \text{sn}^2 \left(\sqrt{p_2/4} |\Omega(N)| t; m \right), \quad (14)$$

where $p_{1,2} = 1 + \frac{\Delta^2}{2|\Omega(N)|^2} \mp \sqrt{\left(1 + \frac{\Delta^2}{2|\Omega(N)|^2}\right)^2 - 1}$, and $m = p_1/p_2$. In Fig. 2, we compare the evolution obtained within our (nonlinear) scheme with that given by the *standard* Rabi model, which is recovered from Eqs. (12) and (13) by replacing the effective coupling constant $\Omega(N)C_A^*$ by $\Omega(N)$. In contrast with the *symmetric* character of the (linear) Rabi oscillations, in the nonlinear case, the oscillations display *asymmetry*. Specifically, because of the incorporation of $C_A(t)$ into the effective interaction strength, the system evolves more slowly as the atomic population decreases. It spends more time *near* the molecular state, where $|C_A| = 0$. In particular, for $\Delta = 0$, and irrespective of the coupling-strength value, the evolution becomes aperiodic: once the system reaches the molecular state, it stays there permanently. In this case, Eq. (14) is simplified to obtain [28, 33]

$$|C_M(t)|^2 = \tanh[|\Omega(N)| t/2], \quad (15)$$

which reflects that, for $E_A = E_M$, there is a complete and *irreversible* transfer of population, as opposed to the oscillations observed in the standard Rabi model. The time needed to complete the process is determined by the coupling strength: larger times are required as $N|\tilde{v}_{eff}|^2$ decreases. This behavior is qualitatively similar to the (*irreversible*) evolution observed for linear ramps. Its persistence in the damped dynamics is the origin of some of the observed features.

The dependence of the period and amplitude of the nonlinear oscillations on $\Omega(N)$ and

Δ can be completely characterized from Eq. (14). Some general properties parallel those corresponding to the linear counterpart. Namely, as $|\Delta|$ grows, the amplitude and the period of the oscillations decrease. (This is illustrated in Figure 3.) Additionally, the amplitude in the nonlinear regime decreases with increasing detuning. Depending on the system dynamics.

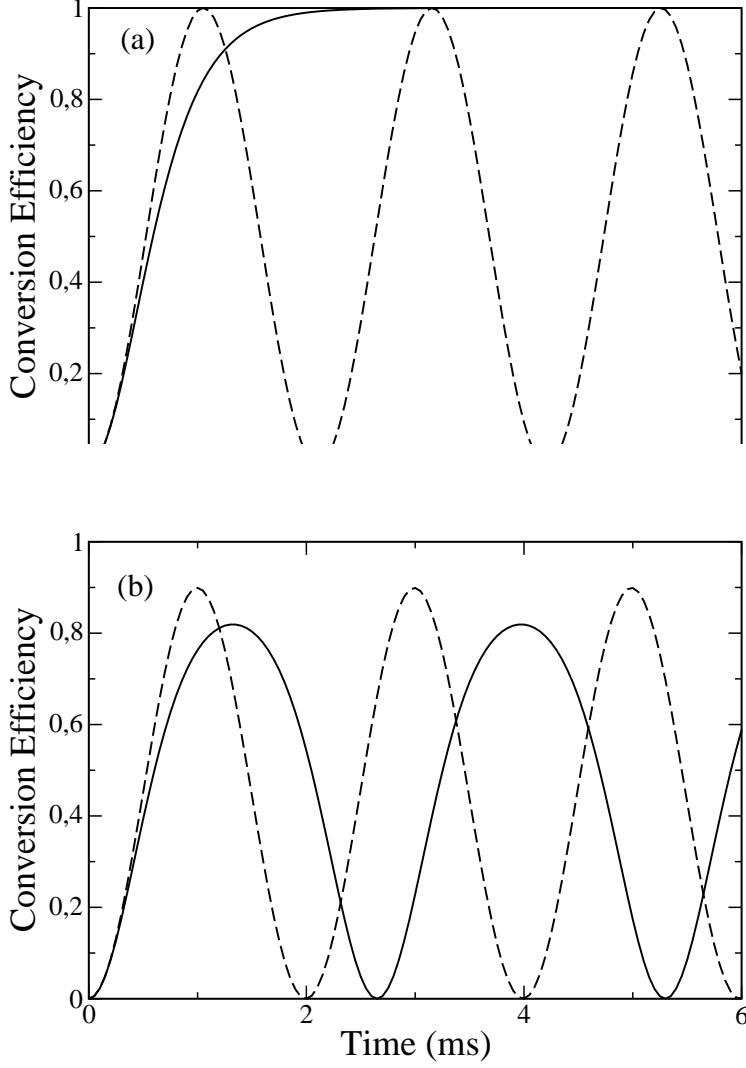


Figure 2: Conversion efficiency $|C_M(t)|^2$ as a function of coupling time, as given by the nonlinear Rabi model [Eqs. (12) and (13) with $\gamma = 0$] (solid line), and by the linear Rabi model (dashed line). The system is prepared in a pure $|A\rangle$ state and two values of the detuning are considered: $\Delta = 0$ (a), and $\Delta = 1$ kHz (b). ($|\Omega(N)| = 3$ kHz).

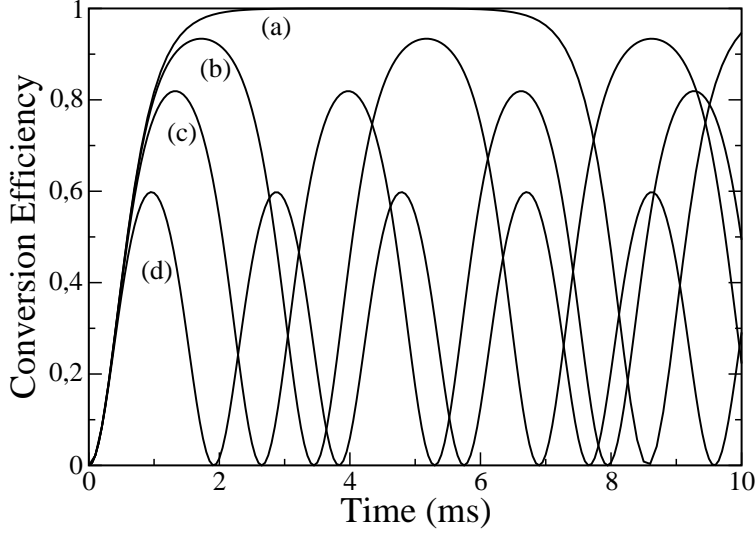


Figure 3: Conversion efficiency $|C_M(t)|^2$ as a function of coupling time, as given by the nonlinear Rabi model [Eqs. (12) and (13) with $\gamma = 0$]. The system is prepared in a pure $|A\rangle$ state and four values of the detuning are considered: $\Delta = 0.01$ kHz (a), $\Delta = 0.5$ kHz (b), $\Delta = 1$ kHz (c), and $\Delta = 2$ kHz (d). ($|\Omega(N)| = 3$ kHz).

B. The role of molecular decay

The occurrence of losses can significantly alter the conversion process. The total population $|C_A(t)|^2 + |C_M(t)|^2$ diminishes as the generated molecules decay and the emerging atoms escape from the trap. The magnitude monitored in the experiments was the difference between the initial atomic population and that corresponding to a generic time, $P_M^{(c)}(t) = 1 - |C_A(t)|^2$ [20], i.e., the sum of the molecular population and the fraction of atoms that have left the trap through molecular decay. In general, the form of $P_M^{(c)}(t)$ can be complex, with different stages and characteristic times. Still, some global properties can be identified. In a simple view, (which will be improved later on with the discussion of the phase-space proximity criterion), one can think that saturation occurs when all the atoms initially present in the trap have disappeared, and, consequently, when the maximum value $P_M^{(c)}(t) = 1$ is attained. Since the atoms escape via transfer to the molecular state and subsequent decay, the scale for saturation depends crucially on the characteristic times of those component processes. Namely, when γ is much larger than the effective conversion rate, the oscillations that could exist in the undamped system are absent, because, once

the molecules are formed, they *suddenly* decay. It is then the transfer that determines the scale for saturation. In the opposite limit, the evolution approaches the undamped oscillations: atom escape can be neglected at times much shorter than $1/\gamma$. The behavior in a general regime incorporates traces of both extreme responses. This is apparent in Fig. 4, where we depict $P_M^{(c)}(t)$ far from the above limits. The displayed features qualitatively reproduce the main experimental findings. A differentiated behavior is associated to $\Delta = 0$, [Fig. 4(a)]: as no oscillations are present, $|C_A(t)|^2$ continuously decreases irrespective of the relative magnitude of the characteristic times for losses and transfer, and, in turn, $P_M^{(c)}(t)$ monotonously grows. In contrast, as shown in Figs. 4(b) and 4(c), various stages appear for $\Delta \neq 0$. Damped oscillations, which are the remnants of the ones existent in the undamped model, can be seen if their period is smaller than $1/\gamma$. The frequency grows with both, the effective coupling strength and $|\Delta|$. Because of the nonzero detuning, no inversion of population takes place; furthermore, for a sufficiently large $|\Delta|$, the amplitude can be much smaller than 1. Once the oscillations have decayed, the monotonous increase of $P_M^{(c)}(t)$ sets in, and the saturation is eventually reached.

Since the appearance of the transitory oscillations demands an appropriate relative magnitude of the partial time scales, their stability can be affected by variations in the number of atoms in the different experimental runs [29]. Actually, the changes in N affect $\Omega(N)$, and, consequently, the Rabi period. The instability associated to thermal effects will be analyzed in the next section.

Our picture applies specifically to the considered detection scheme. A modified approach can be necessary to deal with different arrangements. For instance, a continuous conversion process, which can be implemented via the replacement of the atoms that leave the trap, is described by adding a term of population gain to Eq. (12). The monitored magnitude $P_M^{(c)}(t)$ can then be identified with the molecular population, and the saturation corresponds to the balance between molecule formation and decay [34].

C. The phase-space proximity criterion

In our model, as presented so far, $P_M^{(c)}(t)$ goes to unity, since, after a sufficiently long time, the initial atomic population has disappeared through molecule production and decay. However, in the experiments, the saturation was observed at a value smaller than 1. We can

think of having here a parallel of the reduced efficiency detected in linear-ramp transfers. As, in those processes, the efficiency was found to be determined basically by the density in the phase space, it was argued that a primary requirement for molecule formation could be the proximity of the atoms in position and momentum [35]. This conjecture was validated by the reproduction of the experimental results through a simulation based on a stochastic phase-space sampling with an adjustable cut-off radius limiting the efficient region for association. (Additional support was given via coupled atom-molecule Boltzmann equations [36].) The wide applicability of this criterion [37, 38] seems to convey the generality of the involved mechanisms. Still, the origin of the apparent phase-space depending character of the interaction is not clear [39]. From our approach, some clues to trace it can be given. The efficiency of the conversion depends ultimately on the magnitude of the matrix element $v(E_S) = \langle R|V|S\rangle$ ($E_S = p^2/m$; p denotes the relative linear momentum and m stands for the atom mass.) The variation of $v(E_S)$ with the atom-state characteristics is determined by the overlap between the wave functions $\psi_R(\vec{r}) = \langle \vec{r}|R\rangle$ and $\psi_S^{(p)}(\vec{r}) = \langle \vec{r}|S\rangle$, where \vec{r} denotes the relative coordinate. (Since the operator V accounts for hyperfine interaction between the atom pairs in the open and in the closed channels, it affects only nuclear and electron spin variables, which are fixed in each channel.) The Franck-Condon factor $F(p) \equiv \left| \int d\vec{r} \psi_R^*(\vec{r}) \psi_S^{(p)}(\vec{r}) \right|^2$ can be evaluated under quite general assumptions [40]. It is found that $F(p)$ becomes negligible for values of the momentum larger than $p_L = \hbar/d$, where d represents the size of the bound state. Additionally, $F(p)$ depends linearly on the inverse quantization volume, which implies, in both, condensed and thermal gases, a linear dependence on the density. For a condensate, the linear dependence on N/\mathcal{V} emerges via the incorporation of the amplification factor N into the above expression of $F(p)$; for a thermal gas, the quantization volume in a two-body description is given by the inverse of the density n_T . As the atoms are described in terms of free continuum states, (with phases modified by the scattering), the quantization volume determines the magnitude of the mean atomic distance $\langle S|r|S\rangle$. Hence, the requirement of having a significant Franck-Condon factor can be expressed as a phase-space proximity criterion: for the interaction to be relevant, the atoms must be in states with sufficiently small mean values of position and momentum. This supports the classical formulation of the criterion, namely, $\bar{r} \cdot \bar{p} \leq \frac{\chi}{2} \hbar$, where, \bar{r} and \bar{p} , respectively denote the average relative distance and momentum, and χ is a numerical factor obtained through the optimization of the simulation. From the quantum study, the

magnitude of χ can be estimated via the expression $\langle S|r|S\rangle\langle S|p|S\rangle\sim\frac{\chi}{2}\hbar$, where $|S\rangle$ represents a state that effectively leads to molecular association. Taking $\langle S|p|S\rangle\sim\hbar/d$ and $\langle S|r|S\rangle\sim d$, the magnitude of the obtained value of χ corresponds to that of the classical estimate.

The reduction in the efficiency imposed by the above criterion varies with the temperature and with the character, bosonic or fermionic, of the atomic sample. Here, given the variety of temperatures and condensate fractions realized in the experiments, we take into account the argument of phase-space limitations by considering that only a part of the atoms intervene in the conversion process [35]. As a result, our expression for the efficiency is rewritten as $N_p(1-|C_A(t)|^2)/N_t$, where N_t denotes the initial number of atoms in the system, and N_p corresponds to those that actually take part in the transfer process. In this phenomenological approach, applied to obtain the results of Fig. 4, we can identify the asymptotic efficiency

m

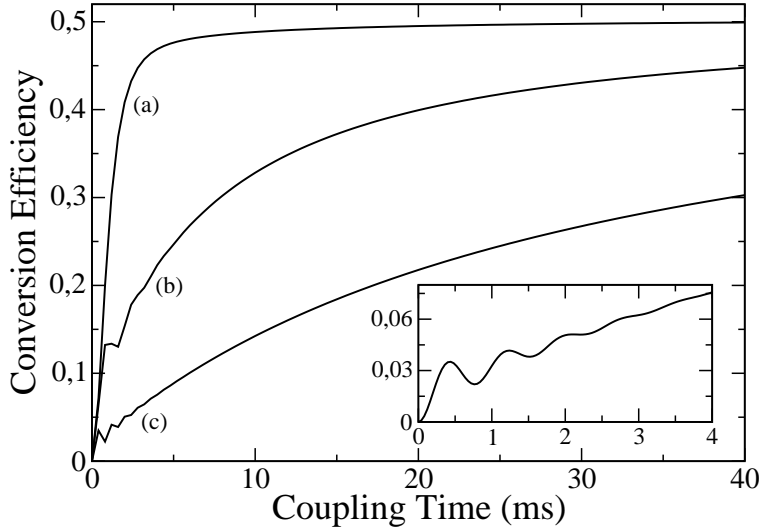


Figure 4: Conversion efficiency $P_M^{(c)}(t)$ as a function of coupling time for the system prepared in pure $|A\rangle$ state for three different values of the detuning: $\Delta = 0$ (a), $\Delta = 2$ kHz (b), and $\Delta = 5$ kHz (c). ($|\Omega(N)| = 3$ kHz, $\gamma = 1$ kHz.) [The inset shows the damped initial-stage oscillations for case (c).] (As in the following figures, the asymptotic efficiency has been arbitrarily fixed.)

IV. THE EFFECT OF THE THERMAL PREPARATION OF THE SYSTEM

We evaluate now the dephasing effects that the system preparation can introduce in the dynamics. The majority of the experiments were done on uncondensed samples [20]. In those arrangements, the starting point was a thermal distribution of atoms at a magnetic-field value far from the FR. At that distance from the resonance, the atom-molecule coupling is practically ineffective, and, consequently, the eigenstates of the complete system are approximately given by the bare states for the initial field. The preparation is then a thermal mixture of $|S\rangle$ states. It can be assumed that, in the first segment of the *trapezoidal* ramp, (Fig. 1), each state $|S\rangle$ adiabatically follows the field, and converts, eventually, into its associated (B_0) dressed state, i.e., into one the states previously denoted as $|A\rangle$. Hence, the initial distribution is transformed into a mixture of $|A\rangle$ states. In the central region, the evolution of the atomic population is calculated applying the standard Rabi model. [The effective coupling constant in Eq. (12) is written as $\tilde{v}_{eff}(n_T)$, since it depends on the atomic density n_T through the quantization volume.] In the last segment of the ramp, the dressed states are adiabatically transformed into their related $|S\rangle$ states.

From the propagation in the *plateau* of each component of the mixture, i.e., of each $|A\rangle$ state, we find $|C_A(t)|^2$. Then, the total atomic population is obtained by averaging $|C_A(t)|^2$ over the Boltzmann distribution of the original mixture of $|S\rangle$ states. The average can be simplified through the following lines. From previous characterizations of the coupling of a discrete level to a quasi-continuum, one can assume that the energy spacing between consecutive states $|A\rangle$ is the same as that existent between their bare counterparts $|S\rangle$. Hence, an appropriate shift in the origin leads the energy E_A of a (generic) $|A\rangle$ state to match the relative kinetic energy p^2/m of the pair of atoms in the original state $|S\rangle$. (Free-space conditions are being used to evaluate the energies and the density of states; p corresponds then to a continuous variable.) Namely, we can write $E_A(p) = p^2/m$, and, in turn, $\Delta(p) = E_M - p^2/m$. Hence, the initial weight function simply corresponds to the Boltzmann distribution for the $|A\rangle$ states with shifted energies. (To indicate that the atomic population $|C_A(t)|^2$ depends on p through $\Delta(p)$, we rewrite it as $|C_A(p, t)|^2$.) Since the statistical average is not affected by the displacement of the energy origin, the total atomic population can be approximated as

$$\rho_{A,A}^{(T)}(t) = \left(\frac{\beta}{\pi m} \right)^{3/2} \int |C_A(p, t)|^2 \exp(-\beta p^2/m) d\vec{p}, \quad (16)$$

where $\beta = (k_B T)^{-1}$. (In the parallel equation for the molecular population, the linear dependence on the atomic density, found in Ref [21] in the short-time limit, becomes apparent.) One can see that the averaging introduces decoherence: the (partial) oscillations present in $|C_A(p, t)|^2$, rooted in nonzero values of $\Delta(p)$, dephase because of the almost continuous variation of $E_A(p)$ along the distribution. Then, in addition to damping generated by losses, there is decoherence due to the preparation of the system, its characteristic time being determined by the width of the distribution, and, therefore, by the temperature. It is also evident that the initial-stage oscillations decay faster as T increases. Moreover, as T is changed, the distribution of detunings is altered, and, as a consequence, the average frequency can be shifted. The time required to reach the saturation regime depends, not only on intrinsic characteristics of the system, but also, on the width of the distribution. These results are illustrated in Figs. 5 and 6, where we represent the efficiency $P_M^{(c)}(t) = 1 - \rho_{A,A}^{(T)}(t)$ for different values of the *threshold* detuning $\Delta(p=0) = E_M = \omega - \epsilon_M$. (From the experimental data, no information can be extracted on the volume and densities, and, therefore, on the effective coupling constants in the condensed and thermal gases; we have used arbitrary values for the coupling constants and the initial distribution of the atomic population. Moreover, equal phase-space densities are considered for the condensed and thermal gases.)

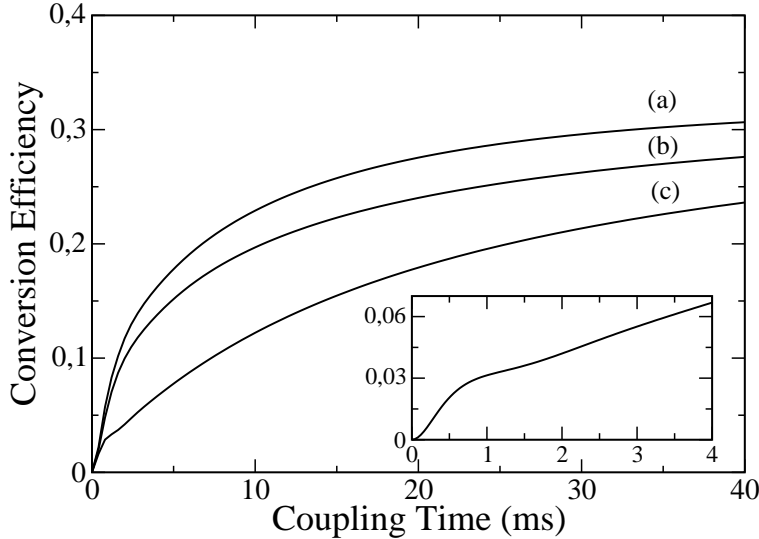


Figure 5: Conversion efficiency $P_M^{(c)}(t)$ as a function of coupling time for the system prepared as a thermal statistical mixture ($T = 20$ mk) for three values of the *threshold* detuning: $\Delta(p = 0) = 5$ kHz (a), $\Delta(p = 0) = 0$ (b), and $\Delta(p = 0) = -2$ kHz (c.) ($\tilde{v}_{eff}(n_T) = 1.5$ kHz, $\gamma = 1$ kHz.) [The in

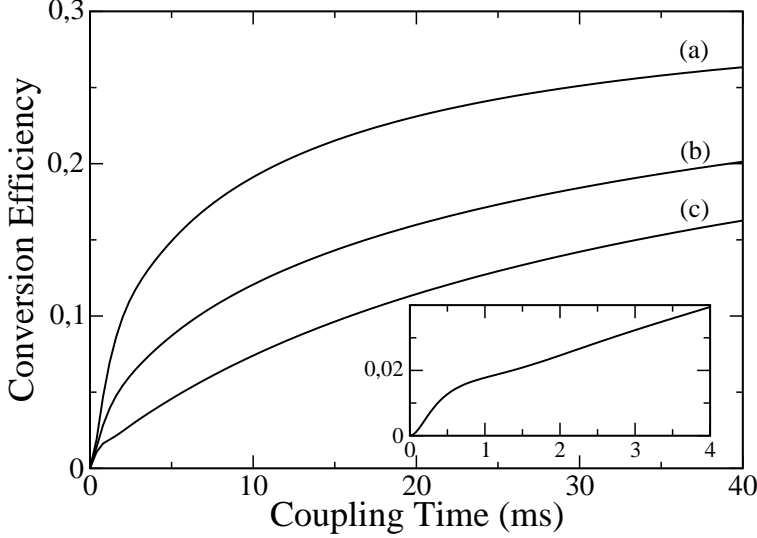


Figure 6: Same caption as Fig. 5 with $T = 40$ mk

Results for the association spectrum, i.e., for the efficiency as a function of the modulation frequency are presented in Ref. [20]. Some of the observed characteristics, like the changing form of the curves at different coupling times or the symmetry properties, must be explained. The multi-factorial character of the dependence of the efficiency on ω is central to the analysis. ω enters the populations through the coupling strength \tilde{v}_{eff} . The detuning, and, therefore, ω , affects also the amplitude of the oscillatory components of the evolution. Moreover, the weights of the statistical mixture effectively modify the amplitudes. To isolate the thermal effects, we have worked with a frequency independent \tilde{v}_{eff} . (In the considered perturbative regime, this is a good approximation, since the factor $J_0(\zeta/\omega)$ does not appreciably differ from unity.) In Figs. 7, 8, and 9, we represent the efficiency as a function of $\Delta = E_M - E_A$ for a pure state, and, of $\Delta(p = 0) = E_M$ for a thermal gas. The magnitude of the used parameters corresponds to the experimental conditions. Apart from common general features, the spectra present differential aspects specific to the preparation characteristics:

i) The resonant behavior observed in the experiments is apparent. For a condensate, (Fig. 7), the resonance occurs at the binding energy. For a thermal gas, (Figs. 8 and 9), as the temperature grows, the resonance is shifted to increasing values of $\Delta(p = 0)$. Actually, in the condensate, the evolution corresponds to just one *oscillatory* term, which reaches its maximum amplitude when $\Delta = 0$. In contrast, for a thermal mixture, there is a quasi-continuous set of oscillatory components in the molecular population. The energy of each state, and, in turn, the corresponding detuning, $\Delta(p)$, vary continuously along the set. Additionally, the statistical weights of the different terms change with the temperature: as T increases, the region of dominant contribution to the integrand in Eq. (16) is shifted to higher E_A . As a consequence, the maximum of the transfer efficiency, which takes place for E_M approximately matching the dominant region of E_A , occurs for higher values of E_M , or, equivalently, for growing detunings.

ii) For the preparation as a condensate, the spectrum is symmetric with respect to the position of the maximum ($\Delta = 0$), since it is the magnitude of the (single) detuning that affects the efficiency. In contrast, there is no symmetry in the thermal case: because of the form of the distribution, the weights of the oscillating terms equidistant from the energy of the maximum are different. One can also understand that the decrease is faster in the region of negative *threshold* detunings, i.e., for effective molecular energies below the atomic set. In those cases, a zero value of $\Delta(p) = E_M - p^2/m$ cannot be reached. Then, there is no component in the mixture attaining its maximum (zero-detuning) amplitude. Moreover, since the magnitude of $\Delta(p)$ monotonously grows along the set, the amplitude of the corresponding oscillatory terms steadily diminishes. Consequently, the output of the transfer is less efficient in that region than in that of positive values of $\Delta(p = 0)$.

iii) The observed time broadening of the spectra is also reproduced: as found in the experiments, the peak width increases with time and eventually saturates. Indeed, as the magnitude of the detuning increases, the conversion becomes less efficient, longer times being needed for molecule formation to take place. Once the asymptotic regime is reached, with all the available atoms converted into molecules, and, afterwards, decaying, the efficiency does not longer increase with time.

Our results reproduce the form of the experimental spectra [20] and coincide with the predictions of previous theoretical work [21].

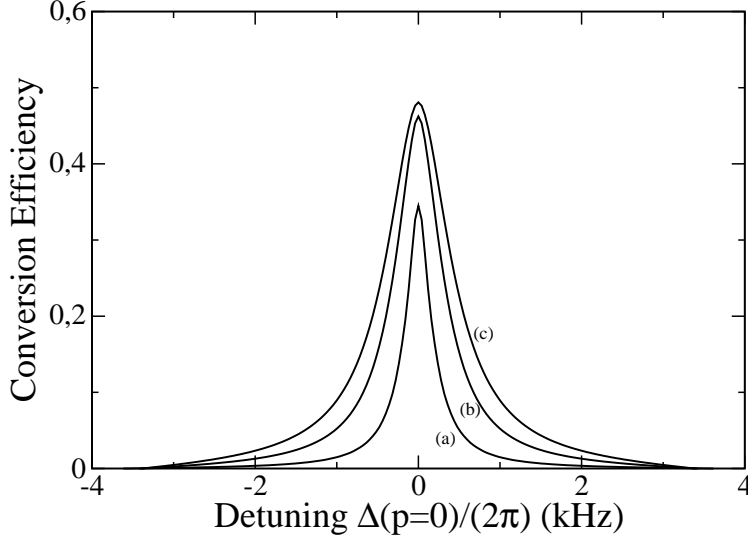


Figure 7: Conversion efficiency $P_M^{(c)}(t)$ as a function of detuning $\Delta/(2\pi)$ for the system prepared in pure $|A\rangle$ state for three coupling times: $t_f = 4$ ms (a), $t_f = 18$ ms (b), and $t_f = 34.4$ ms (c).

(1)

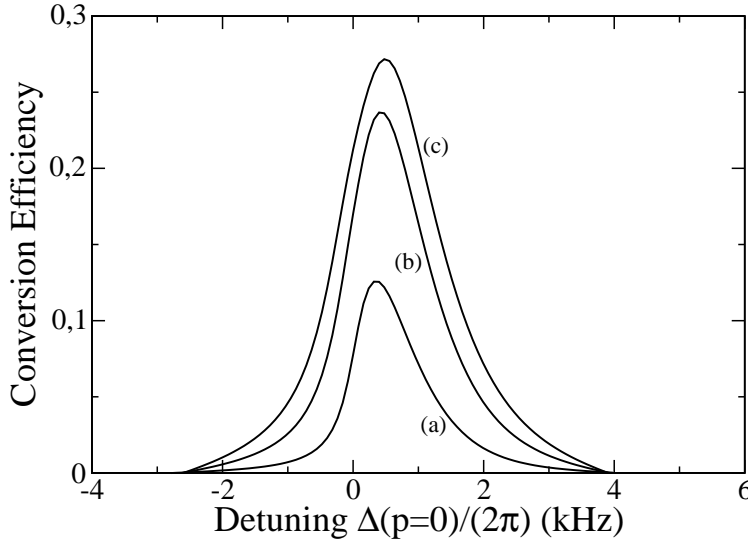


Figure 8: Conversion efficiency $P_M^{(c)}(t)$ as a function of *threshold* detuning $\Delta(p=0)/(2\pi)$ for the system prepared as a thermal statistical mixture ($T = 20$ mk) for three coupling times: $t_f = 4$ ms (a), $t_f = 18$. ms (b), and $t_f = 34.4$ ms (c). ($\tilde{\nu}_{eff}(n_T) = 0.9$ kHz, $\gamma = 1$ kHz.)

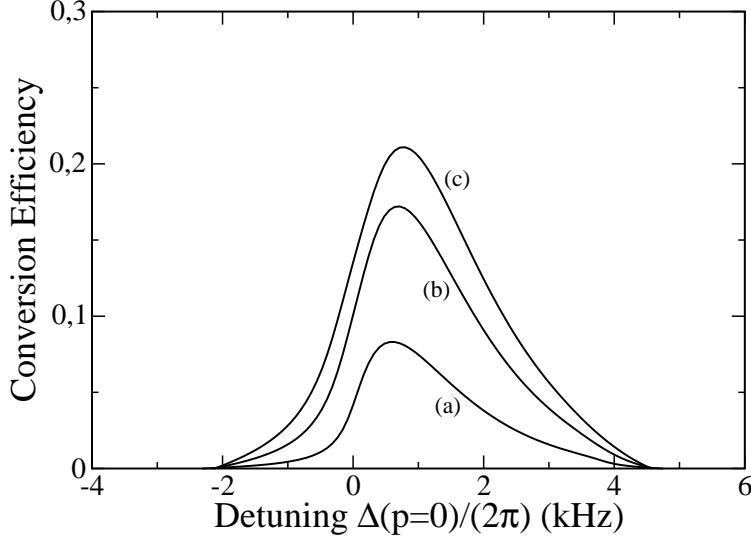


Figure 9: Same caption as Fig. 8 with $T = 40$ mk

V. CONCLUDING REMARKS

Our analysis opens the possibility of controlling the response of the system to the applied field. The partial analytical character of the results facilitates the design of strategies for improving the molecule production. The effective interaction strength can be regarded as a parameter of control. Appropriate modifications of it, through variations of the modulation characteristics, can be implemented to optimize the efficiency or to reduce the transfer time. One can also think of using a different confinement, (e.g., trapping in an optical lattice instead of the original harmonic potential), to have an additional element of control to vary the coupling matrix element and to reduce or suppress inelastic collisions.

The analysis, although focused on a particular method of ultracold molecule production, can have general implications as it deals with fundamental mechanisms. In this sense, the identification of the role of the different components of the dynamics can give some clues to the description of related systems. The intended operative character of the study has implied simplifications in the presentation and tracing of our approach. We project a more complete account of the derivation of the model from a microscopic description. Another objective of future work is the evaluation in different contexts of our conjectures on the basic

mechanisms that can limit the efficiency.

- [1] For a review, see T. Kohler, K. Goral, and P. Julienne, *Rev. Mod. Phys.* **78**, 1311 (2006); and references therein.
- [2] E. A. Donley, N. R. Claussen, S. T. Thomson, and C. E. Wieman, *Nature (London)* **417**, 529 (2002).
- [3] C. A. Regal, C. Ticknor, J. L. Bohn, and D. S. Jin, *Nature (London)* **424**, 47 (2003).
- [4] K. E. Strecker, G. B. Partridge, and R. G. Hulet, *Phys. Rev. Lett.* **91**, 080406 (2003).
- [5] H.R. Thorsheim, J. Weiner, and P.S. Julienne, *Phys. Rev. Lett.* **58**, 2420 (1987).
- [6] K. Winkler, G. Thalhammer, M. Theis, H. Ritsch, R. Grimm, and J. H. Denschlag, *Phys. Rev. Lett.* **95**, 063202 (2005).
- [7] T. Rom, T. Best, O. Mandel, A. Widera, M. Greiner, T. W. Hansch, and I. Bloch, *Phys. Rev. Lett.* **93**, 073002 (2004).
- [8] M. Greiner, C. A. Regal, and D. S. Jin, *Nature (London)* **426**, 537 (2003).
- [9] J. Cubizolles, T. Bourdel, S. J. J. M. F. Kokkelmans, G. V. Shlyapnikov, and C. Salomon, *Phys. Rev. Lett.* **91**, 240401 (2003).
- [10] K. Xu, T. Mukaiyama, J. R. Abo-Shaeer, J. K. Chin, D. E. Miller, and W. Ketterle, *Phys. Rev. Lett.* **91**, 210402 (2003).
- [11] T. Mukaiyama, J. R. Abo-Shaeer, K. Xu, J. K. Chin, and W. Ketterle, *Phys. Rev. Lett.* **92**, 180402 (2004).
- [12] J. Herbig, T. Kraemer, M. Mark, T. Weber, C. Chin, H.-C. Nagerl, and R. Grimm, *Science* **301**, 1510 (2003).
- [13] S. Dürr, T. Volz, A. Marte, and G. Rempe, *Phys. Rev. Lett.* **92**, 020406 (2004).
- [14] S. Jochim, M. Bartenstein, A. Altmeyer, G. Hendl, S. Riedl, C. Chin, J. Hecker-Denschlag, and R. Grimm, *Science* **302**, 2101 (2003).
- [15] M. Bartenstein, A. Altmeyer, S. Riedl, S. Jochim, C. Chin, J. Hecker-Denschlag, and R. Grimm, *Phys. Rev. Lett.* **92**, 120401 (2004).
- [16] C. A. Regal, M. Greiner, and D. S. Jin, *Phys. Rev. Lett.* **92**, 040403 (2004).
- [17] T. Volz, S. Dürr, N. Syassen, G. Rempe, E. van Kempen, and S. Kokkelmans, *Phys. Rev. A* **72**, 010704 (2005).

- [18] K. Goral, T. Kohler, and K. Burnett, Phys. Rev A **71**, 023603 (2005).
- [19] M. L. Olsen, J. D. Perreault, T. D. Cumby, and D. S. Jin, Phys. Rev A, **80**, 030701R (2009).
- [20] S. T. Thomson, E. Hodby, and C. E. Wieman, Phys. Rev. Lett. **95**, 190404 (2005).
- [21] T. M. Hanna, T. Kohler, and K. Burnett, Phys. Rev A **75**, 013606 (2007).
- [22] J. F. Bertelsen and K. Molmer, Phys. Rev A **73**, 013811 (2006).
- [23] C. Weber, G. Barontini, J. Catani, G. Thalhammer, M. Inguscio, and F. Minardi, Phys. Rev. A **78**, 061601 (2008).
- [24] P. Dyke, S. E. Pollack, and R. G. Hulet, Phys. Rev. A **88**, 023625 (2013).
- [25] Landau, L. D., 1932, Phys. Z. Sowjetunion **2**, 46; C. Zener, Proc. R. Soc. A **137**, 696 (1932).
- [26] F. H. Mies, E. Tiesinga, and P. S. Julienne, Phys. Rev A **61**, 022721 (2000).
- [27] K. Goral, T. Kohler, S. A. Gardiner, E. Tiesinga, and P. Julienne, J. Phys. B **37**, 3457 (2004).
- [28] I. S. Gradshteyn and I. M. Ryshik, *Table of Integrals, Series, and Products* (Academic Press, New York, 1994).
- [29] S. T. Thomson, *Dissertation Thesis*, University of Colorado, (2006).
- [30] C. Cohen-Tannoudji and P. Avan, Colloq. Int. C.N.R.S. **273**, 93 (1977); C. Cohen-Tannoudji, J. Dupont-Roc, and G. Grynberg, *Atom-Photon Interactions* (John Wiley & Sons, Inc., New York, 1992).
- [31] S. T. Thomson, E. Hodby, and C. E. Wieman, Phys. Rev. Lett. **94**, 020401 (2005).
- [32] E. Timmermans, P. Tommasini, M. Hussein, and A. Kerman, Phys. Rep. **315**, 199 (1999).
- [33] A. Ishkhanyan, G. P. Chernikov, and H. Nakamura, Phys. Rev. A **70**, 053611 (2004).
- [34] C.-H. Wu, J. W. Park, P. Ahmadi, S. Will, and M. W. Zwierlein, Phys. Rev. Lett. **109**, 085301 (2012).
- [35] Hodby, E., S. T. Thompson, C. A. Regal, M. Greiner, A. C. Wilson, D. S. Jin, E. A. Cornell, and C. E. Wieman, Phys. Rev. Lett. **94**, 120402 (2005).
- [36] J. E. Williams, N. Nygaard, and C. W. Clark, New J. Phys. **8**, **150** (2006).
- [37] Mi Yan, B. J. DeSalvo, Ying Huang, P. Naidon, and T. C. Killian, Phys. Rev. Lett. **111**, 150402 (2013).
- [38] T. D. Cumby, R. A. Shewmon, M.-G. Hu, J. D. Perreault, and D. S. Jin, Phys. Rev. A **87**, 012703 (2013).
- [39] J. J. Zirbel, K.-K. Ni, S. Ospelkaus, T. L. Nicholson, M. L. Olsen, P. S. Julienne, C. E. Wieman, J. Ye, and D. S. Jin, Phys. Rev. A **78**, 013416 (2008).

- [40] W. Ketterle and M. W. Zwierlein, Proceedings of the International School of Physics "Enrico Fermi", Course CLXIV, (IOS Press, Amsterdam, 2008), and references therein.